Chiral electron transport: Scattering through helical potentials

Sina Yeganeh,[1] Mark A. Ratner,[1,a)] Ernesto Medina,[2] and Vladimiro Mujica[1,3,b)]
[1]*Department of Chemistry and Center for Nanofabrication and Molecular Self-Assembly, Northwestern University, Evanston, Illinois 60208-3113, USA*
[2]*Laboratorio de Física Estadística de Sistemas Desordenados, Centro de Física, IVIC, Apartado 21827, Caracas 1020A, Venezuela*
[3]*Argonne National Laboratory, Center for Nanoscale Materials, Argonne, Illinois 60439-4831, USA*

(Received 20 March 2009; accepted 10 June 2009; published online 7 July 2009)

We present a model for the transmission of spin-polarized electrons through oriented chiral molecules, where the chiral structure is represented by a helix. The scattering potential contains a confining term and a spin-orbit contribution that is responsible for the spin-dependent scattering of electrons by the molecular target. The differential scattering cross section is calculated for right- and left-handed helices and for arbitrary electron spin polarizations. We apply our model to explain chiral effects in the intensity of photoemitted polarized electrons transmitted through thin organic layers. These are molecular interfaces that exhibit spin-selective scattering with surprisingly large asymmetry factors as well as a number of remarkable magnetic properties. In our model, differences in intensity are generated by the preferential transmission of electron beams whose polarization is oriented in the same direction as the sense of advance of the helix. This model can be easily extended to the Landauer regime of conductance where conductance is due to elastic scattering, so that we can consider the conductance of chiral molecular junctions. © *2009 American Institute of Physics*. [DOI: 10.1063/1.3167404]

I. INTRODUCTION

Chirality in chemical systems presents a broken symmetry which can be probed in combination with another symmetry breaking operation. If we ignore the extremely small effects of parity violation,[1–5] polarized light,[6] magnetic field,[7] or spin-polarized electrons (SPEs) (Ref. 8) are the obvious means to yield different interactions with mirror-image isomers. SPEs are of particular interest[9] since their interaction with chiral molecular targets can provoke measurable changes in the spin polarization.[10] These SPEs can be produced by shining circularly polarized light on gaseous metal atoms[11] or, more commonly, on solids.[12,13] In both cases, excitations to the continuum are perturbed by spin-orbit (SO) coupling, yielding selective spin orientation.[11,14]

Electron spin polarization[15] has been used to probe the effects of scattering of electron beams by chiral molecules. In analogy to the differential absorption of polarized light by chiral molecules in optical dichroism experiments, the differential scattering of polarized electrons has been termed electron dichroism. In particular, Farago and co-workers[8,16,17] instigated the study of electron scattering from D/L-camphor molecules and found small effects in the electron polarization and beam attenuation for scattered electrons. Later, Mayer and Kessler verified the existence of electron dichroism in bromocamphor with asymmetries around 1 in 10^4.[18] Thompson and co-workers[19–23] pointed out that even unpolarized electrons will scatter differently from oriented chiral molecules in cases where the experimental geometry establishes the necessary chiral interaction. For the most part, the magnitude of these chiral effects has been small due to the low atomic number in the systems examined and small SO coupling.

These experiments have examined molecules that possess point chirality at carbon centers; we, however, focus on helical systems with axial chirality. In recent years, Naaman and co-workers examined the scattering of polarized electrons from thin films of chiral molecules on gold surfaces.[24–27] In these experiments, circularly polarized light is shined on the gold substrate upon which molecules with point or axial chirality (helices) are adsorbed. SPEs are produced, and the transmission of these electrons is measured for left-/right-handed circularly polarized light and hence parallel/antiparallel longitudinally polarized spins as well as for mirror-image molecules. They have found surprisingly large asymmetry factors in the electron transmission for up and down spins for chiral systems (as large as 1 in 10). They ascribe the larger-than-expected magnitude of this asymmetry to cooperative effects in the monolayer.[28,29]

In this paper, we argue that the origin of this large asymmetry is partly due to a combination of the presence of the molecule with axial chirality (providing a mechanism for larger SO interaction than expected with only point chirality for low atomic number systems),[30] orientation on the surface,[20] and cooperative effects in the monolayer. In a future paper we will address the last factor, but here we focus on describing polarized electron transmission through an oriented helix. This relates to previous work examining magnetochiral anisotropy in nanotubes,[31–34] but we do not consider the effect of magnetic field. Instead, beginning with a simple model for a free electron on a helix[31,35] we apply scattering theory to derive the differential cross section. We focus here

a)Electronic mail: ratner@northwestern.edu.
b)Electronic mail: vmujica@northwestern.edu.

on the scattering experiments of Naaman and co-workers, although tunneling experiments with chiral systems have also been reported.[27] Our scattering theory results also provide an approach for understanding chiral effects in molecular junctions[36–38] within the Landauer limit[39] where electron transport can be considered purely as a scattering process. The interaction of spin polarization and chirality also suggests a link with work in molecular spintronics.[40–43]

II. SCATTERING THEORY

A. Formalism

We present here a brief background to the scattering theory of polarized electrons as necessary for our work. There is an important literature on the subject that includes the books by Sitenko[44] and Kessler[14] and numerous papers from the past three decades[1,10,15,17–23] to mention some of the most relevant work.

A general framework for the description of the spin-dependent elastic scattering of polarized electrons requires the use of density matrix formalism because mixed states of arbitrary polarization cannot be described using wave functions which are only appropriate for pure spin states.[14,44,45] The density matrix $\boldsymbol{\rho}$ and the spin-dependent scattering amplitude $\mathbf{f}$ can be written as linear combinations of the 2×2 unit matrix $\mathbf{1}$ and the Pauli matrices $\boldsymbol{\sigma}=(\sigma_x,\sigma_y,\sigma_z)$:

$$\boldsymbol{\rho}=a\mathbf{1}+\mathbf{b}\cdot\boldsymbol{\sigma}, \tag{1}$$

$$\mathbf{f}=g\mathbf{1}+\mathbf{h}\cdot\boldsymbol{\sigma}, \tag{2}$$

where a, $\mathbf{b}$, g, and $\mathbf{h}$ describe the various scattering processes and their spin dependencies. Since the scattering amplitude and the density matrix must be invariant with respect to rotations and reflections of the coordinate system and the spin $\boldsymbol{\sigma}$ is a pseudovector, it follows based on general symmetry arguments that a and g must be scalars while $\mathbf{b}$ and $\mathbf{h}$ are pseudovectors. These quantities will in general depend on the initial and final states, the geometry of the collision between the polarized electron beam and the molecule, and the nature of the interaction.

The density matrix of the system after scattering $\boldsymbol{\rho}'$ can then be expressed as

$$\boldsymbol{\rho}'=\mathbf{f}\boldsymbol{\rho}\mathbf{f}^{\dagger}, \tag{3}$$

and the spin-polarization vector $\mathbf{P}$ is written simply in terms of the spin density matrix as

$$\mathbf{P}=\frac{\mathrm{Tr}(\boldsymbol{\sigma}\boldsymbol{\rho})}{\mathrm{Tr}\,\boldsymbol{\rho}}. \tag{4}$$

For an incident unpolarized beam the density matrix is given by $\boldsymbol{\rho}=\frac{1}{2}\mathbf{1}$. The scattering amplitude matrix $\mathbf{f}$ is not unitary, and for the problem of one-electron scattering considered below it is related to the transition operator matrix $\mathbf{t}$ by[44]

$$\mathbf{f}_{\sigma,\sigma'}(\mathbf{k}_a,\mathbf{k}_b)=-\frac{\mu}{2\pi\hbar^2}\langle\mathbf{k}_a\sigma'|\mathbf{t}|\mathbf{k}_b\sigma\rangle, \tag{5}$$

where $\mathbf{k}_{a,b}$ give the electron trajectory before and after scattering and μ is the reduced mass. For arbitrary i initial and f final states the unitary S-matrix $\mathbf{S}$ corresponding to the full space-spin description of the elastic scattering process is related to the $\mathbf{t}$-matrix in the energy shell by

$$-2\pi i\mathbf{t}_{fi}\delta(E_f-E_i)=\mathbf{S}_{fi}-\mathbf{1}. \tag{6}$$

It follows from Eq. (3) that the final polarization depends on the initial state and that even if the initial beam is completely unpolarized, the final state can be polarized due to the nonunitary character of $\mathbf{f}$.[44] In general, the final polarization will depend on both the preparation of the initial state and the scattering potential. As discussed in the work of Blum and Thompson,[19] spin-dependent scattering can occur even for achiral molecules provided that the molecules are oriented in a well-defined way with respect to the polarization vector. In the experiments of Naaman and co-workers, molecules are adsorbed on a gold surface which provides a natural orientation. Polarized electrons are produced in the surface by exciting with circularly polarized photons. The partial transfer of angular momentum from the photons to the electrons produces spin polarization, and as recognized early on by Fano[11] this process cannot occur in the absence of SO interaction. In our theoretical model, we assume that there is an orientation of the chiral molecules in the adlayer and that initial state preparation has produced a state with well-defined polarization vector.

B. The importance of chirality

A crucial point for understanding the experiments of Naaman and co-workers is that the observed electron dichroism depends strongly on the chiral nature of the molecules in the monolayer and that it is essentially absent either if the purity of the enantiomer present in the layer is reduced by even small quantities (i.e., 1% in some of their experiments) or if an achiral species is used.[24] To describe this observed electron dichroism, we rewrite the spin-dependent scattering amplitude [Eq. (2)] as[1,10,21]

$$\mathbf{f}=g\mathbf{1}+h_1\mathbf{n_1}\cdot\boldsymbol{\sigma}+h_2\mathbf{n_2}\cdot\boldsymbol{\sigma}+h_3\mathbf{n_3}\cdot\boldsymbol{\sigma}, \tag{7}$$

where the unit vectors $\mathbf{n_1}$, $\mathbf{n_2}$, and $\mathbf{n_3}$ are defined by

$$\mathbf{n_1}=\frac{\mathbf{k}_b+\mathbf{k}_a}{|\mathbf{k}_b+\mathbf{k}_a|},\quad \mathbf{n_2}=\frac{\mathbf{k}_b-\mathbf{k}_a}{|\mathbf{k}_b-\mathbf{k}_a|},\quad \mathbf{n_3}=\frac{\mathbf{k}_a\times\mathbf{k}_b}{|\mathbf{k}_a\times\mathbf{k}_b|}, \tag{8}$$

and the vector $\mathbf{h}$ has been expanded in terms of these vectors and the parameters $h_{1,2,3}$. The g and h_3 terms are present for both chiral and achiral species, while h_1 and h_2 are nonzero only for chiral systems and form the basis for the treatment of chiral scattering.

We now narrow our discussion to consider the elastic scattering of spin-quantized electrons from a helical potential with explicit consideration of the SO interaction. For this case we can explicitly calculate the scattering matrix. The scattering potential consists of two parts describing the spatial part of the potential $V(r)$ and the SO interaction H_{SO}:[46]

$$V(r,\hat{\sigma})=V(r)+H_{\mathrm{SO}}(r,\hat{\sigma}), \tag{9}$$

$$H_{\mathrm{SO}}=-\alpha\hat{\sigma}\cdot[\nabla\hat{V}\wedge\mathbf{p}], \tag{10}$$

where α quantifies the effective strength of the SO coupling and $\mathbf{p}$ is the momentum. For the bare SO interaction (in

vacuum) $\alpha=-\hbar/(2m_e c)^2$, where m_e is the electron mass and c the speed of light. In many applications of atomic and molecular physics, where the effective electron-nucleus interaction can be represented by a central potential, the strength of the SO coupling is simply proportional to the atomic number Z of the heaviest nucleus, and the SO Hamiltonian can be written in terms of the electronic angular momentum $\mathbf{L}$ and spin $\mathbf{S}$ as

$$H_{\mathrm{SO}} = \xi(r)\boldsymbol{L}\cdot\boldsymbol{S}, \tag{11}$$

where the effective coupling constant is given by

$$\xi(r) = \frac{Ze^2\hbar^2}{2\mu^2c^2r^3}. \tag{12}$$

The form of H_{SO} in Eq. (10) is similar to that of the Rashba Hamiltonian where the α is proportional to the field strength. It describes the spin splitting of energy bands in semiconductors in the presence of an external field.[47] In the Rashba case, the α factor depends on the microscopic SO interaction, the band structure, and the gradient of the potential. Compared to the atomic case described by Eq. (11), in the crystalline environment the SO parameter can be enhanced by two mechanisms:[48] (i) in the absence of strong electric fields and because the relevant electrons are at the Fermi level, the electron velocities can be of the order of 10^8 cm/s, enhancing the SO interaction by way of its momentum dependence; (ii) the second mechanism is by means of the implied dipole moments introduced by the lack of inversion symmetry in highly anisotropic structures. Both effects will induce a strong SO interaction even at low potential gradients, well beyond the vacuum values. A coarse order-of-magnitude comparison can be drawn from the fact that the α factor in Eq. (10) is inversely proportional to the electron rest mass, in the MeV, while the gap in semiconductors is only in the eV, rendering an effect that could be 10^6 larger.[49] A similar argument has been given for tunneling in molecular layers where effective electron masses one order of magnitude smaller than m_e have been estimated.[50,51] This would translate into an effective coupling that is two orders of magnitude larger than the bare Dirac SO coupling.

To describe a right-handed helix aligned along the z-axis we write in parametric form:[35]

$$\begin{aligned} x &= a\cos\varphi, \\ y &= a\sin\varphi, \\ z &= b\varphi, \\ V(x,y,z) &= \begin{cases} V_0 & \text{for } 0 \le \varphi \le 2\pi K \\ 0 & \text{otherwise.} \end{cases} \end{aligned} \tag{13}$$

In the above equations, a is the radius of the helix, $2\pi b$ is the pitch, K is the number of turns, and V_0 is the magnitude of the scattering potential (constant along the helix). φ represents the position along the helix. For a left-handed helix, the definitions of x and y are switched (or $\varphi\rightarrow-\varphi$).

The scattering Schrödinger equation can be written as

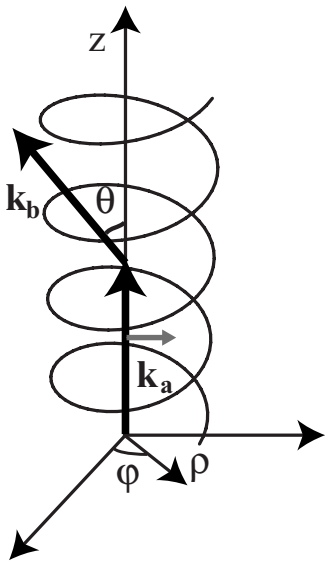

FIG. 1. The proposed scattering geometry is diagrammed. The photoemitted electron is produced upon absorption of circularly polarized light traveling parallel to the long axis (z) of the helix with its spin quantized along the same direction.

$$(\nabla^2 + k^2)\Psi = \frac{2\mu}{\hbar}V(r,\hat{\sigma})\Psi, \tag{14}$$

where $\hbar k$ is the relative momentum of the scattering electron and the helix and $\mu \approx m_e$ is the reduced mass of the system. $\Psi=\psi\chi_{m_s}$, where ψ is the spatial part of the wave function, and χ_{m_s} is a spin function with $S=1/2$ and $m_s=\pm 1/2$. We take as our initial state the spin-polarized plane wave,

$$\Phi_a = e^{ik_a r}\chi_{m_s}, \tag{15}$$

and we assume, based on experimental reports,[24] that spin polarization lies along the same axis as the helix ($\hat{\boldsymbol{z}}$) (Fig. 1). At large distances from the scattering event and in the first Born approximation (FBA), we can write the solution for the (not normalized) scattered wave function as

$$\Psi = \Phi_a + F_{m_s}\frac{e^{ikr}}{r}, \tag{16}$$

where F_{m_s}, the scattering amplitude, is given in FBA by[46]

$$\begin{aligned} F_{m_s} &= -\frac{\mu}{2\pi\hbar^2}\int e^{-i\mathbf{k}_b\cdot\mathbf{r}'}V(\mathbf{r}',\hat{\sigma})e^{i\mathbf{k}_a\cdot\mathbf{r}'}d^3\mathbf{r}'\chi_{m_s} \\ &= -\frac{\mu}{2\pi\hbar^2}(A+B)\chi_{m_s}, \end{aligned} \tag{17}$$

with

$$A = \int e^{-i\mathbf{k}_b\cdot\mathbf{r}'}V(\mathbf{r}')e^{i\mathbf{k}_a\cdot\mathbf{r}'}d^3\mathbf{r}', \tag{18}$$

$$B = \alpha\int e^{-i\mathbf{k}_b\cdot\mathbf{r}'}\hat{\sigma}\cdot[\nabla\hat{V}\wedge\mathbf{p}]e^{i\mathbf{k}_a\cdot\mathbf{r}'}d^3\mathbf{r}'. \tag{19}$$

In the above equations, $\mathbf{k}_{a,b}$ once again define the electron trajectory before and after scattering with $|\mathbf{k}_a-\mathbf{k}_b| = 2k\sin(\theta/2)$, where θ is the scattering angle. Note that F_{m_s}

is a spinor, and so in general we expect that for a given initial state ($\chi_{\pm 1/2}$) there will be both spin-maintaining and spin-flipping contributions to the scattering amplitude. The differential cross section for the spin-polarized case is then given by

$$\frac{d\sigma}{d\Omega} = |F_{m_s}|^2, \tag{20}$$

and for the unpolarized case

$$\frac{d\sigma}{d\Omega}^{\text{unpolarized}} = \frac{1}{2}\sum_{m_s} |F_{m_s}|^2. \tag{21}$$

We also define Ξ, a quantity that describes the amount of asymmetry induced by spin polarization from scattering through the helix and SO interaction:

$$\Xi = \frac{\left| \frac{d\sigma}{d\Omega}^{\uparrow} - \frac{d\sigma}{d\Omega}^{\downarrow} \right|}{\frac{d\sigma}{d\Omega}^{\text{unpolarized}}}. \tag{22}$$

We now evaluate the integrals in Eqs. (18) and (19). The repulsive helix potential can be written as

$$\begin{aligned} V(\mathbf{r}) &= V_0 \delta^3(\mathbf{r} - a(\hat{\mathbf{x}} \cos\varphi + \hat{\mathbf{y}} \sin\varphi) \pm \hat{\mathbf{z}} b\varphi) \\ &= \frac{V_0}{2\pi\rho}\delta(\rho - a)\delta(z \pm b\varphi), \end{aligned} \tag{23}$$

where the $\pm$ refers to left-/right-handed helices. The delta function has been redefined in cylindrical coordinates. We will later rewrite the variable vectors $\hat{\boldsymbol{\varphi}}$ and $\hat{\boldsymbol{\rho}}$ in fixed Cartesian coordinates using $\hat{\boldsymbol{\varphi}} = -\hat{\mathbf{x}} \sin\varphi + \hat{\mathbf{y}} \cos\varphi$ and $\hat{\boldsymbol{\rho}} = \hat{\mathbf{x}} \cos\varphi + \hat{\mathbf{y}} \sin\varphi$. We can write the integral A (with volume element $\rho d\rho d\varphi dz$) as

$$A = \frac{V_0}{2\pi}\int\int\int e^{i(\mathbf{k}_a - \mathbf{k}_b)\cdot\mathbf{r}'}\delta(\rho - a)\delta(z \pm b\varphi) d\rho d\varphi dz. \tag{24}$$

We write $\mathbf{r}' = \rho\hat{\boldsymbol{\rho}} + z\hat{\mathbf{z}}$, and we take the incident plane wave to be in the $\hat{z}$ direction, parallel to the helix axis, so that $\mathbf{k}_a = k\hat{\mathbf{z}}$ (we assume elastic scattering so that k is preserved). We can then write the integrand as

$$\begin{aligned} A &= \frac{V_0}{2\pi}\int\int\int e^{ikz} e^{-ik\rho\sin\theta} e^{-ikz\cos\theta} \\ &\quad \times \delta(\rho - a)\delta(z \pm b\varphi) d\rho d\varphi dz \\ &= \frac{V_0}{2\pi}\int_{-\infty}^{\infty} dz \int_0^{2\pi K} d\varphi e^{ikz(1-\cos\theta)}\delta(z \pm b\varphi) \\ &\quad \times \int_0^{\infty} d\rho e^{-ik\rho\sin\theta}\delta(\rho - a) \\ &= \pm \frac{V_0}{2\pi} \frac{e^{-ika\sin\theta}}{ikb(1 - \cos\theta)}[e^{\pm 2\pi i K k b(1-\cos\theta)} - 1]. \end{aligned} \tag{25}$$

Note that in the absence of SO coupling ($B=0$), the differential cross section is proportional to $|A|^2$, and the scattering is the same for right-/left-handed helices. There is also no spin dependence, as expected.

Now approaching integral B that describes the SO effect, we write

$$\begin{aligned} \nabla\hat{V} &= \nabla\frac{V_0}{2\pi\rho}\delta(\rho - a)\delta(z \pm b\varphi) \\ &= \left(\hat{\boldsymbol{\rho}}\frac{\partial}{\partial\rho} + \hat{\boldsymbol{\varphi}}\frac{1}{\rho}\frac{\partial}{\partial\varphi} + \hat{z}\frac{\partial}{\partial z}\right)\frac{V_0}{2\pi\rho}\delta(\rho - a)\delta(z \pm b\varphi) \\ &= \frac{V_0}{2\pi\rho}\left[\hat{\boldsymbol{\rho}}\left[\delta'(\rho - a) - \frac{1}{\rho}\delta(\rho - a)\right]\delta(z \pm b\varphi)\right. \\ &\quad \pm \hat{\boldsymbol{\varphi}}\frac{1}{\rho}\delta(\rho - a)\delta'(z \pm b\varphi)b \\ &\quad \left. + \hat{z}\delta(\rho - a)\delta'(z \pm b\varphi)\right] \end{aligned} \tag{26}$$

to be used in the expression

$$B = -\hbar\alpha\int e^{-i\mathbf{k}_b\cdot\mathbf{r}'}\hat{\boldsymbol{\sigma}}\cdot[\nabla\hat{V} \wedge i\nabla]e^{i\mathbf{k}_a\cdot\mathbf{r}'}d^3\mathbf{r}', \tag{27}$$

where we have used $\mathbf{p} = (\hbar/i)\nabla$. Operating with the momentum operator on the incident plane wave yields

$$B = \hbar\alpha\int e^{-i\mathbf{k}_b\cdot\mathbf{r}'}\hat{\boldsymbol{\sigma}}\cdot[\nabla\hat{V} \wedge \mathbf{k}_a]e^{i\mathbf{k}_a\cdot\mathbf{r}'}d^3\mathbf{r}'. \tag{28}$$

We now evaluate the wedge product between the gradient of the potential and momentum vector, $\mathbf{k}_a = k\hat{\mathbf{z}}$, to obtain

$$\begin{aligned} \nabla V \wedge k\hat{\mathbf{z}} = \frac{V_0}{2\pi\rho}k\left[-\hat{\boldsymbol{\varphi}}\left[\delta'(\rho - a) - \frac{1}{\rho}\delta(\rho - a)\right]\right. \\ \left.\times\delta(z \pm b\varphi) \pm \hat{\boldsymbol{\rho}}\frac{1}{\rho}\delta(\rho - a)\delta'(z \pm b\varphi)b\right]. \end{aligned} \tag{29}$$

Once again $e^{i(\mathbf{k}_a - \mathbf{k}_b)\cdot\mathbf{r}'} = e^{ikz(1-\cos\theta)}e^{-ik\rho\sin\theta}$. The integral for B can then be written as

$$\begin{aligned} B = \hbar\alpha\frac{V_0}{2\pi}k\hat{\boldsymbol{\sigma}}\cdot\int\int\int e^{ikz(1-\cos\theta)}e^{-ik\rho\sin\theta} \\ \times\left[-\hat{\boldsymbol{\varphi}}\left[\delta'(\rho - a) - \frac{1}{\rho}\delta(\rho - a)\right]\delta(z \pm b\varphi)\right. \\ \left.\pm\hat{\boldsymbol{\rho}}\frac{1}{\rho}\delta(\rho - a)\delta'(z \pm b\varphi)b\right]d\rho d\varphi dz. \end{aligned} \tag{30}$$

As we integrate over $d\varphi d\rho dz$, we now rewrite the variable vectors $\hat{\boldsymbol{\varphi}}$ and $\hat{\boldsymbol{\rho}}$ in fixed Cartesian coordinates using $\hat{\boldsymbol{\varphi}} = -\hat{\mathbf{x}}\sin\varphi + \hat{\mathbf{y}}\cos\varphi$ and $\hat{\boldsymbol{\rho}} = \hat{\mathbf{x}}\cos\varphi + \hat{\mathbf{y}}\sin\varphi$. The doublet functions are evaluated with $\int\delta'(x-a)f(x)dx = -f'(a)$.

For simplicity we write

$$B = \hbar\alpha\frac{V_0}{2\pi}k\hat{\boldsymbol{\sigma}}\cdot(\mathbf{I}_{\varphi} + \mathbf{I}_{\rho}). \tag{31}$$

First, we address the integral proportional to $\hat{\varphi}$:

$$\mathbf{I}_\varphi = \int\int\int e^{ikz(1-\cos\theta)} e^{-ik\rho\sin\theta}(-\hat{\boldsymbol{\varphi}})\left[\delta'(\rho-a) - \frac{1}{\rho}\delta(\rho-a)\right]\delta(z \pm b\varphi)d\rho d\varphi dz = \int_{-\infty}^{\infty} dz \int_0^{2\pi K} d\varphi e^{ikz(1-\cos\theta)}\delta(z \pm b\varphi)$$
$$\times(\hat{\mathbf{x}}\sin\varphi - \hat{\mathbf{y}}\cos\varphi)\int_0^{\infty} d\rho e^{-ik\rho\sin\theta}\left[\delta'(\rho-a) - \frac{1}{\rho}\delta(\rho-a)\right] = \left[ik\sin\theta\, e^{-ika\sin\theta} - \frac{e^{-ika\sin\theta}}{a}\right]\int_0^{2\pi K} d\varphi e^{\pm ikb\varphi(1-\cos\theta)}$$
$$\times(\hat{\mathbf{x}}\sin\varphi - \hat{\mathbf{y}}\cos\varphi). \tag{32}$$

The last two integrals are easily found:

$$S_1 = \int_0^{2\pi K} d\varphi e^{\pm ikb\varphi(1-\cos\theta)}\sin\varphi = \frac{e^{\pm 2\pi i\lambda K}}{\lambda^2-1}(\cos 2\pi K \mp i\lambda \sin 2\pi K - e^{\mp 2\pi i\lambda K}), \tag{33}$$

$$C_1 = \int_0^{2\pi K} d\varphi e^{\pm ikb\varphi(1-\cos\theta)}\cos\varphi = \frac{ie^{\pm 2\pi i\lambda K}}{\lambda^2-1}(\mp\lambda\cos 2\pi K + i\sin 2\pi K \pm \lambda e^{\mp 2\pi i\lambda K}), \tag{34}$$

where we have defined $\lambda = kb(1-\cos\theta)$ for simplicity. We thus have

$$\mathbf{I}_\varphi = \left[ik\sin\theta e^{-ika\sin\theta} - \frac{e^{-ika\sin\theta}}{a}\right](\hat{\mathbf{x}}S_1 - \hat{\mathbf{y}}C_1). \tag{35}$$

We next address the integral proportional to $\hat{\boldsymbol{\rho}}$:

$$\mathbf{I}_\rho = \int\int\int e^{ikz(1-\cos\theta)} e^{-ik\rho\sin\theta}\left[\pm\hat{\boldsymbol{\rho}}\frac{1}{\rho}\right.$$
$$\left.\times\delta(\rho-a)\delta'(z \pm b\varphi)b\right]d\rho d\varphi dz$$
$$= \pm\int_{\infty}^{\infty} dz\int_0^{2\pi K} d\varphi e^{ikz(1-\cos\theta)}\delta'(z \pm b\varphi)(\hat{\mathbf{x}}\cos\varphi$$
$$+ \hat{\mathbf{y}}\sin\varphi)b\int_0^{\infty} d\rho\frac{e^{-ik\rho\sin\theta}}{\rho}\delta(\rho-a)$$
$$= \mp\frac{i\lambda}{a}e^{-ika\sin\theta}(\hat{\mathbf{x}}C_1 + \hat{\mathbf{y}}S_1). \tag{36}$$

Finally, we can write the full B integral as

$$B = \hbar\alpha\frac{V_0}{2\pi}k\hat{\boldsymbol{\sigma}}\cdot\left[\left(ik\sin\theta\, e^{-ika\sin\theta} - \frac{e^{-ika\sin\theta}}{a}\right)\right.$$
$$\left.\times(\hat{\mathbf{x}}S_1 - \hat{\mathbf{y}}C_1) \mp \left(\frac{i\lambda}{a}e^{-ika\sin\theta}\right)(\hat{\mathbf{x}}C_1 + \hat{\mathbf{y}}S_1)\right]. \tag{37}$$

In Sec. III, we will use these expressions for A [Eq. (25)] and B [Eq. (37)] with Eqs. (20)–(22) to estimate the magnitude of chiral effects expected in electron tunneling through helical systems.

III. RESULTS AND DISCUSSION

Using the scattering theory results from above, we can examine the magnitude of the chiral effect. For a reasonable set of helix parameters (V_0, a, b, K), the differential cross section as well as Ξ can be calculated. We begin by rewriting Eq. (17):

$$F_{m_s} = -\frac{\mu}{2\pi\hbar^2}(A\mathbf{1} + \hat{\boldsymbol{\sigma}}\cdot(B_x\hat{\mathbf{x}} + B_y\hat{\mathbf{y}}))\chi_{m_s}, \tag{38}$$

where $B_{x,y}$ are the terms proportional to $\hat{\mathbf{x}}$ and $\hat{\mathbf{y}}$ in Eq. (37). From here we can write the different scattering amplitudes for $\chi_{\pm 1/2}$:

$$F_{+1/2} = -\frac{\mu}{2\pi\hbar^2}\begin{pmatrix} A \\ B_x + iB_y\end{pmatrix}, \tag{39}$$

$$F_{-1/2} = -\frac{\mu}{2\pi\hbar^2}\begin{pmatrix} B_x - iB_y \\ A\end{pmatrix}, \tag{40}$$

as well as the differential cross section:

$$\frac{d\sigma}{d\Omega}_{\uparrow} = \left(\frac{\mu}{2\pi\hbar^2}\right)^2(|A|^2 + |B_x + iB_y|^2), \tag{41}$$

$$\frac{d\sigma}{d\Omega}_{\downarrow} = \left(\frac{\mu}{2\pi\hbar^2}\right)^2(|A|^2 + |B_x - iB_y|^2), \tag{42}$$

$$\frac{d\sigma}{d\Omega}_{\text{unpolarized}} = \left(\frac{\mu}{2\pi\hbar^2}\right)^2(2|A|^2 + |B_x + iB_y|^2 + |B_x - iB_y|^2)/2, \tag{43}$$

where we have squared and then summed the spinor components since in the spin-dependent transmission experiments only the intensity of photoemitted electrons is measured, and all outgoing spin information is discarded. We now can clearly see the effect of the chiral interaction on the scattering event; the same-spin component of the scattering amplitude is proportional to A, but with the inclusion of SO coupling there is also a smaller but potentially significant contribution to the spin-flipping component from the B terms. Note that since $B_{x,y}$ are complex quantities, the spin-up and spin-down cross sections will in general differ.

The asymmetry factor can thus be rewritten:

$$\Xi = \frac{||B_x + iB_y|^2 - |B_x - iB_y|^2|}{(2|A|^2 + |B_x + iB_y|^2 + |B_x - iB_y|^2)/2}. \quad (44)$$

We can readily appreciate here the importance of chirality in obtaining a finite value for Ξ. Setting the pitch of the helix b to zero eliminates chirality and although $F_{+1/2}$ and $F_{-1/2}$ differ, their modulus square is identical, yielding $\Xi=0$, as can be seen from Eq. (44). The crux of the spin-flipping mechanism is the change in the incident k vector of the electron. This generates an orbital angular momentum that must be compensated for by a change in spin. We can restate this argument in a very general way. The total angular momentum of the incident electron is given by $\mathbf{J}=\mathbf{r}\times\mathbf{p}+\mathbf{s}$ where $\mathbf{r}$ is the position with respect to some origin, $\mathbf{p}$ is the electron momentum, and $\mathbf{s}$ is the spin angular momentum. Taking the time derivative of the total angular momentum, setting $\dot{\mathbf{J}}=0$ (by angular momentum conservation), and assuming elastic scattering we arrive at the condition

$$\dot{\mathbf{s}} + \dot{\mathbf{r}} \times \mathbf{p} = -\mathbf{r} \times \dot{\mathbf{p}}. \quad (45)$$

This has the essence of a conservation equation[52–54] for the angular momentum involving the change in spin angular momentum and the divergence of a material spin current which is nonzero due to the SO term in the Hamiltonian. On the right-hand side of Eq. (45) is a torque, related to the change in momentum during the scattering as argued above. *However*, this is not enough to generate a net spin polarization! For an axially symmetric scatterer, i.e., a circular ring with $b=0$ in our nomenclature, these angular momentum transfers average out, yielding no scattering differences between up and down spins. It is the pitch magnitude and sign that yield different differential cross sections. This is the most obvious argument that chirality must enter as a spin-flipping mechanism.

In Fig. 2, we have plotted Ξ for reasonable helix parameters and given SO coupling strength. With the bare SO coupling, the effect of chirality on the spin asymmetry is very small (1 part in 10^6 at most), as expected from the electron dichroism experiments of gas-phase molecules. However, if the SO coupling is enhanced by effective mass effects, as have been reported in tunneling measurements through Langmuir–Blodgett films,[55] one could obtain $\alpha=(10-10^4)\times\hbar/(2m_ec)^2$ and we could see substantial spin asymmetries in certain regimes. In particular, for large scattering angles and high kinetic energy electrons, Ξ is found to be quite large, with values between 1 part in 100 and 1. In Fig. 3, we focus on the effect of altering helix pitch on Ξ and verify the importance of helicity for the chiral effect. As the pitch b of the helix becomes small compared to the radius a, the potential becomes a circular ring, and the chiral effect disappears as expected. At very large values of b the potential becomes a straight line, and the effect disappears as well. Additionally, our model predicts a nonobvious dependence of the chiral effect on the length (number of turns) of the helix. Because of the cancellation of constructive/destructive interferences, the scattering asymmetries for $K=K+n$ are equal for $n\in\mathbb{Z}$.

To compare more explicitly with experiment, we integrate the differential cross section over scattering angles to yield Ξ as a function of electron energy. We assume that all

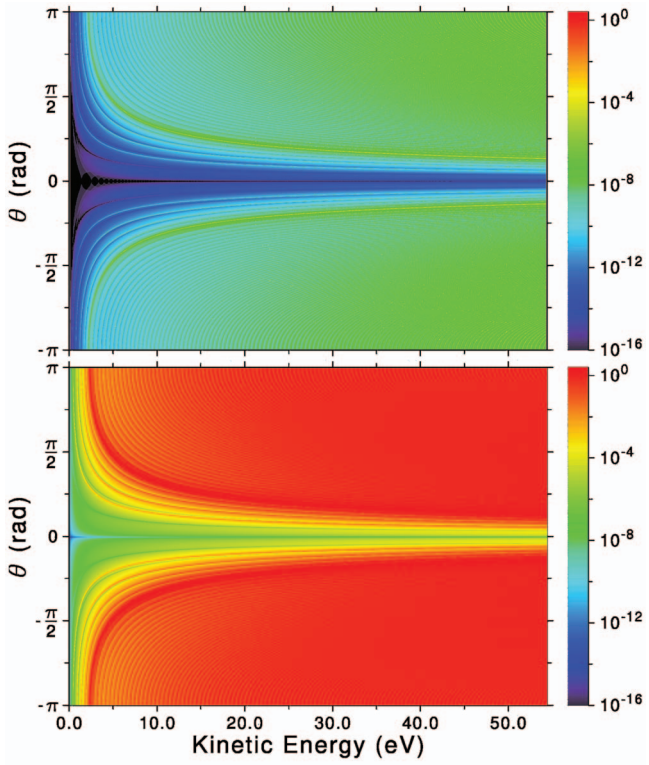

FIG. 2. The spin-polarization ratio Ξ as defined in Eqs. (22) and (44) is plotted for a right-handed helix as a function of the kinetic energy of the incoming particles and the scattering angle θ. $V_0=1$ eV, $a=1$ Å, $b=3$ Å, and $K=5.1$ turns, and the spin-quantization axis is along the helix axis ($\hat{\mathbf{z}}$). Above, the bare SO coupling is taken, $\alpha=-\hbar/(2m_ec)^2$, and below an effective SO coupling is used, $\alpha=-2\times10^4\hbar/(2m_ec)^2$. The results for a left-handed helix are identical.

electrons scattered forward between $-\pi$ and π are detected by the experimental setup. The result is shown in Fig. 4. At the experimental kinetic energies (around 1 eV), the asymmetry is small, but at higher kinetic energies, even the integrated asymmetry factor can be substantial. In one particular experimental system with double-stranded DNA on gold,[24] the spin selectivity was found to be roughly 50%. Our calculations indicate smaller values for the chiral asymmetry, on the order of 10% (at much higher kinetic energies than in experiment). The crude treatment of the molecular potential and the assumption of elastic scattering in our model might be the source of the discrepancy in the kinetic energy necessary for the chiral effect to appear as well the difference in magnitude.

Looking at the analytic forms for the spin-maintaining (A) and spin-flipping (B) contributions to the scattering amplitude, we see that in general $F^{\uparrow}_{m_s=+1/2}=F^{\downarrow}_{m_s=-1/2}$, i.e., the spin-maintaining parts (proportional to A) are equal for both incoming spin polarizations even in a chiral system with polarized electrons. In the presence of nonzero SO coupling, however, the spin-flip amplitudes will differ, $F^{\downarrow}_{m_s=+1/2} \neq F^{\uparrow}_{m_s=-1/2}$. Regardless of the value of α, for a right-handed helix with the parameters we take in Figs. 2 and 4, we find the magnitude of $F^{\downarrow}_{m_s=+1/2}$ to be roughly 10^3 times larger than that of $F^{\uparrow}_{m_s=-1/2}$. In other words, when the spin is aligned "towards" the forward scattering direction there is a significantly enhanced spin-flip contribution compared to when the

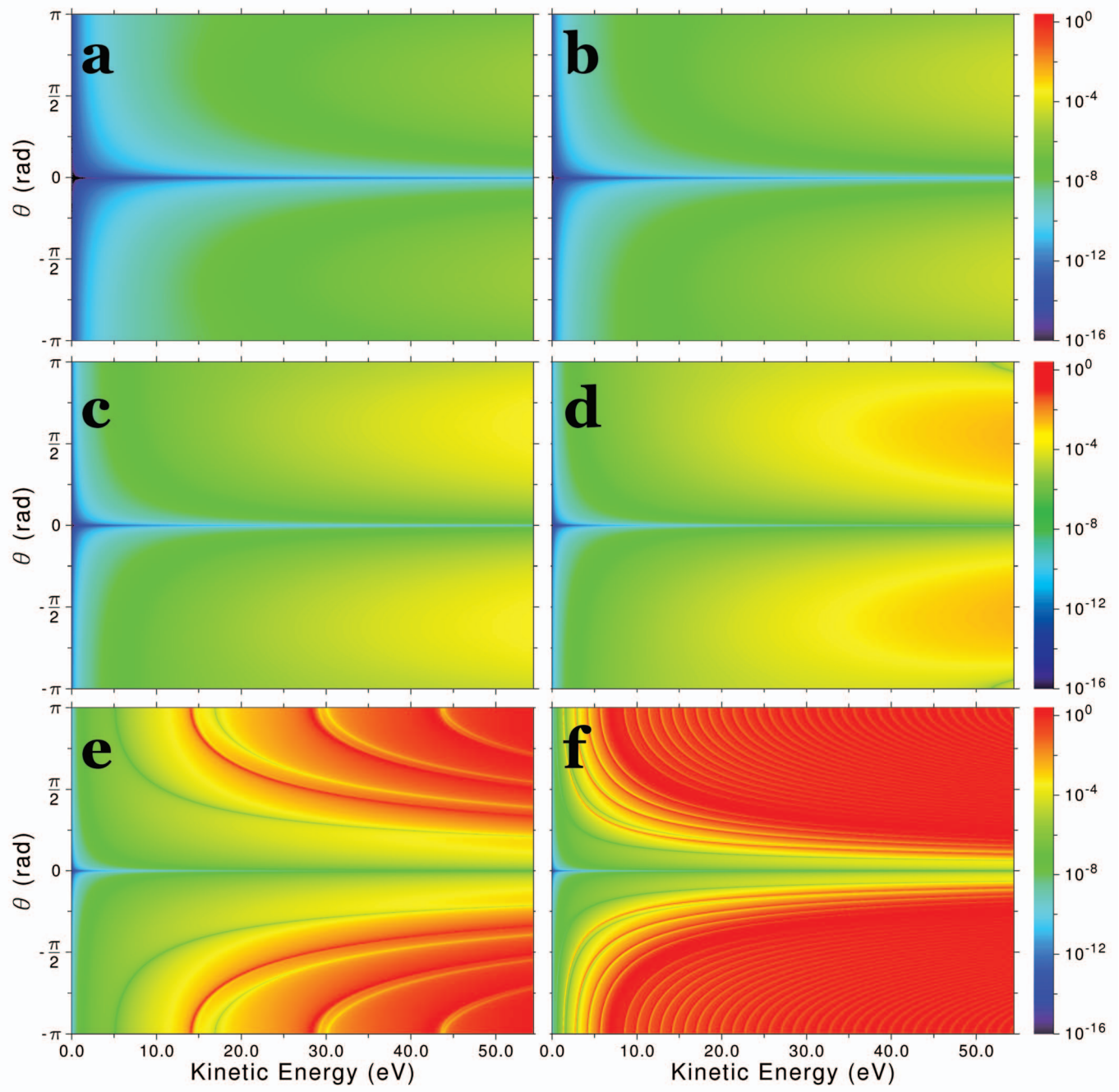

FIG. 3. Ξ is plotted for a number of different values for the helix pitch b. In all plots, $V_0=1$ eV, $a=1$ Å, and $K=5.1$. The spin-quantization axis is along the helix axis, and the effective SO coupling is taken to be $\alpha=-2\times10^4\hbar/(2m_ec)^2$. In (a), $b=10^{-5}$ Å; in (b), $b=10^{-4}$ Å; in (c), $b=10^{-3}$ Å; in (d), $b=10^{-2}$ Å; in (e), $b=10^{-1}$ Å; in (f), $b=10^{0}$ Å. As the ratio b/a increases, the potential changes from a ring to a helix, and the magnitude of the asymmetry factor increases.

spin is aligned "opposite" the forward direction. This relation is reversed for a left-handed helix. This we posit is the source of the asymmetry in transmission through chiral films. Of course, the relative magnitudes of spin-maintaining and spin-flipping amplitudes will determine the relevance of this effect; for bare SO coupling, the spin flip is only 10^{-9} the value of the spin-maintaining contribution. However, with monolayer enhancement, we propose that the SO coupling can be enhanced (as in Fig. 4) and as a result spin flipping can be 10^{-1} the value of the spin-maintaining contribution.

As noted in Sec. II, polarized electron transmission in chiral organic monolayers is extremely sensitive to disorder. This is in sharp contrast to the situation in optical dichroism where the optical activity of a mixture of enantiomers is simply a sum of algebraic contributions of each optical isomer. The marked dependence on disorder suggests that the problem is related to quantum interference, and this argument has been used in the context of gas-phase electron scattering by ensembles of molecules.[56] Another intriguing aspect of transmission experiments, also related to disorder sensitivity, is the estimation of the number of molecules in the monolayer that are sampled during the scattering event. These types of collective effects as well as the inclusion of localized magnetic moments in the surface-monolayer inter-

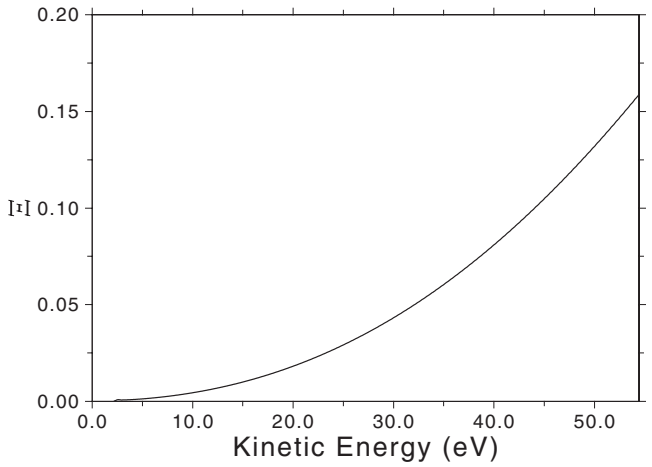

FIG. 4. The spin-polarization ratio Ξ (integrated over forward scattering angles from $-\pi$ to π) is plotted with the same helix parameters as in Fig. 2. The effective SO coupling is taken to be $\alpha=-2\times10^4\hbar/(2m_ec)^2$. Although not shown, at higher kinetic energies the plot plateaus.

face are currently under investigation as there is strong evidence that these types of excitations are responsible for some of the remarkable magnetic properties of these systems.[24,57]

In a recent article by Skourtis *et al.*,[58] the argument of path interference has been invoked in explaining how a difference in electron transfer rates for right- and left-handed enantiomers of a molecule can arise. In this very relevant work there is no inclusion of spin and SO interactions that we believe are important ingredients in understanding the behavior of spin-active interfaces like those considered in this work. A more comprehensive model of these systems should probably include the arguments of Skourtis *et al.* as well as those presented here and, in addition, an appropriate description of the local magnetic fields associated with the interface.

In the low voltage (off-resonant) regime of molecular electronics, the scattering theory treatment developed in this paper can be inserted into the Landauer expression for the current. Our results predict that in true single-molecule devices (e.g., break junction experiments) chiral effects will be negligible; however, the work of Naaman and co-workers suggest that in molecular junctions formed from chiral monolayers, there is the real possibility of observing chiral effects if magnetic scanning tunneling microscopy[59] is used as a source of SPEs.

ACKNOWLEDGMENTS

We thank G. Solomon, T. Hansen, and A. Nitzan for helpful discussions. S.Y. is grateful for support from the Office of Naval Research through a NDSEG fellowship. We thank the NSF for support from the Division of Chemistry as well as the Division of Materials Research through the Northwestern MRSEC.

[1] P. S. Farago, J. Phys. B **13**, L567 (1980).
[2] R. A. Hegstrom, J. Mol. Struct.: THEOCHEM **232**, 17 (1991).
[3] R. A. Hegstrom, D. W. Rein, and P. G. H. Sandars, J. Chem. Phys. **73**, 2329 (1980).
[4] D. W. Walker, J. Phys. B **15**, L289 (1982).
[5] A. Rich, J. Vanhouse, and R. A. Hegstrom, Phys. Rev. Lett. **48**, 1341 (1982).
[6] E. U. Condon, W. Altar, and H. Eyring, J. Chem. Phys. **5**, 753 (1937).
[7] M. E. Pospelov, Phys. Lett. A **220**, 194 (1996).
[8] D. M. Campbell and P. S. Farago, Nature (London) **318**, 52 (1985).
[9] J. Kirschner, *Polarized Electrons at Surfaces*, Springer Tracts in Modern Physics Vol. 106 (Springer-Verlag, Berlin, 1985).
[10] K. Blum and D. G. Thompson, Adv. At., Mol., Opt. Phys. **38**, 39 (1998).
[11] U. Fano, Phys. Rev. **178**, 131 (1969).
[12] G. Borstel and M. Wöhlecke, Phys. Rev. B **26**, 1148 (1982).
[13] Linearly polarized light could, however, produce SPEs in noncentrosymmetric solids as discussed in Ref. 12.
[14] J. Kessler, *Polarized Electrons* (Springer-Verlag, Berlin, 1985).
[15] P. S. Farago, Rep. Prog. Phys. **34**, 1055 (1971).
[16] D. M. Campbell and P. S. Farago, J. Phys. B **20**, 5133 (1987).
[17] P. S. Farago, J. Phys. B **14**, L743 (1981).
[18] S. Mayer and J. Kessler, Phys. Rev. Lett. **74**, 4803 (1995).
[19] K. Blum and D. Thompson, J. Phys. B **22**, 1823 (1989).
[20] A. Busalla, K. Blum, and D. G. Thompson, Phys. Rev. Lett. **83**, 1562 (1999).
[21] C. Johnston, K. Blum, and D. Thompson, J. Phys. B **26**, 965 (1993).
[22] M. Musigmann, A. Busalla, K. Blum, and D. G. Thompson, J. Phys. B **34**, L79 (2001).
[23] D. G. Thompson, Can. J. Phys. **74**, 920 (1996).
[24] K. Ray, S. P. Ananthavel, D. H. Waldeck, and R. Naaman, Science **283**, 814 (1999).
[25] S. G. Ray, S. S. Daube, G. Leitus, Z. Vager, and R. Naaman, Phys. Rev. Lett. **96**, 036101 (2006).
[26] Z. Vager, I. Carmeli, G. Leitus, S. Reich, and R. Naaman, J. Phys. Chem. Solids **65**, 713 (2004).
[27] J. J. Wei, C. Schafmeister, G. Bird, A. Paul, R. Naaman, and D. H. Waldeck, J. Phys. Chem. B **110**, 1301 (2006).
[28] D. Cahen, R. Naaman, and Z. Vager, Adv. Funct. Mater. **15**, 1571 (2005).
[29] Z. Vager and R. Naaman, Chem. Phys. **281**, 305 (2002).
[30] F. Kuemmeth, S. Ilani, D. C. Ralph, and P. L. McEuen, Nature (London) **452**, 448 (2008).
[31] V. Krstic and G. L. J. A. Rikken, Chem. Phys. Lett. **364**, 51 (2002).
[32] V. Krstic, S. Roth, M. Burghard, K. Kern, and G. L. J. A. Rikken, J. Chem. Phys. **117**, 11315 (2002).
[33] V. Krstic, G. Wagniere, and G. L. J. A. Rikken, Chem. Phys. Lett. **390**, 25 (2004).
[34] Y. Miyamoto, S. G. Louie, and M. L. Cohen, Phys. Rev. Lett. **76**, 2121 (1996).
[35] I. Tinoco and R. W. Woody, J. Chem. Phys. **40**, 160 (1964).
[36] A. Aviram and M. A. Ratner, Chem. Phys. Lett. **29**, 277 (1974).
[37] D. Bloor, *Introduction to Molecular Electronics* (Oxford Univerity Press, New York, 1995), Chap. 1, pp. 1–28.
[38] F. L. Carter, J. Vac. Sci. Technol. B **1**, 959 (1983).
[39] M. Buttiker, Y. Imry, R. Landauer, and S. Pinhas, Phys. Rev. B **31**, 6207 (1985).
[40] E. G. Emberly and G. Kirczenow, Chem. Phys. **281**, 311 (2002).
[41] M. Zwolak and M. Di Ventra, Appl. Phys. Lett. **81**, 925 (2002).
[42] R. Liu, S. H. Ke, W. Yang, and H. U. Baranger, J. Chem. Phys. **127**, 141104 (2007).
[43] S. Datta and B. Das, Appl. Phys. Lett. **56**, 665 (1990).
[44] A. G. Sitenko, *Lectures in Scattering Theory* (Pergamon, Oxford, 1971).
[45] K. Blum, *Density Matrix Theory and Applications* (Plenum, New York, 1996).
[46] A. S. Davydov, *Quantum Mechanics* (Pergamon, Oxford, 1965).
[47] E. I. Rashba, Sov. Phys. Solid State **2**, 1109 (1960).
[48] E. I. Rashba, Physica E (Amsterdam) **20**, 189 (2004).
[49] R. Winkler, *Spin-Orbit Coupling Effects in Two Dimensional Electron Hole Systems* (Springer-Verlag, Berlin, 2003).
[50] W. Y. Wang, T. Lee, and M. A. Reed, Phys. Rev. B **68**, 035416 (2003).
[51] C. Joachim and M. Magoga, Chem. Phys. **281**, 347 (2002).
[52] S. Murakami, N. Nagaosa, and S. C. Zhang, Science **301**, 1348 (2003).
[53] P. Q. Jin, Y. Q. Li, and F. Zhang, J. Phys. A **39**, 7115 (2006).

[54] E. Medina, A. Lopez, and B. Berche, Europhys. Lett. **83**, 47005 (2008).
[55] H. J. Che, P. J. Chia, L. L. Chua, S. Sivaramakrishnan, J. C. Tang, A. T. Wee, H. S. Chan, and P. K. Ho, Appl. Phys. Lett. **92**, 253503 (2008).
[56] D. G. Thompson and M. Kinnin, J. Phys. B **28**, 2473 (1995).
[57] C. Gonzalez, Y. Simon-Manso, M. Marquez, and V. Mujica, J. Phys. Chem. B **110**, 687 (2006).
[58] S. Skourtis, D. Beratan, R. Naaman, A. Nitzan, and D. H. Waldeck, Phys. Rev. Lett. **101**, 238103 (2008).
[59] S. Krause, L. Berbil-Bautista, G. Herzog, M. Bode, and R. Wiesendanger, Science **317**, 1537 (2007).